Characterization of a Diiron(III) Peroxo Intermediate in the Reaction Cycle of Methane Monooxygenase Hydroxylase from *Methylococcus capsulatus* (Bath)

Katherine E. Liu,[†] Ann M. Valentine,[†] Di Qiu,[‡] Dale E. Edmondson,[§] Evan H. Appelman,[⊥] Thomas G. Spiro,*[,‡] and Stephen J. Lippard*[,†]

Departments of Chemistry
Massachusetts Institute of Technology
Cambridge, Massachusetts 02139
Princeton University
Princeton, New Jersey 08540
Department of Biochemistry, Emory University
Atlanta, Georgia 30322
Chemistry Division, Argonne National Laboratory
Argonne, Illinois 60439

Received November 22, 1994

Methane monooxygenase (MMO) is a multicomponent enzymatic system which catalyzes the conversion of methane to methanol.[1] The diiron(II) state of the hydroxylase component (H_{red}) of soluble MMO in the presence of protein B activates dioxygen for substrate hydroxylation.[2,3] Previously, two intermediates were described for the reaction of dioxygen with H_{red} and protein B from *Methylococcus capsulatus* (Bath)[4] and *Methylosinus trichosporium* OB3b.[5,6] Kinetic parameters from optical stopped-flow and rapid freeze-quench Mössbauer data revealed that H_{red} reacts rapidly with dioxygen ($k \approx 20-25\ s^{-1}$) to form the first observed intermediate, which is more slowly ($k \approx 0.3-1\ s^{-1}$) converted to the second.[4,6] Decay of the latter proceeds with concomitant production of alcohol and H_{ox}. The Mössbauer parameters for both intermediates are unusual and do not match the values of any structurally characterized carboxylate-bridged diiron model compounds.[4,5] The second intermediate exhibits a low isomer shift in the range 0.14−0.21 mm/s[4,5] and has been assigned as an Fe(IV) species.[5] Based on an isomer shift of 0.66 mm/s, three possible assignments for the first intermediate were considered:[4] a diiron(III) peroxide, a superoxide anion radical coordinated to an Fe(II)-Fe(III) center, and an antiferromagnetically coupled dioxygen adduct of an intermediate spin diiron(II) unit. In the present Communication, we present new optical and resonance Raman spectroscopic data that characterize the first intermediate as a diiron(III) peroxo species.

Native H_{ox} (diiron(III) form) or H_{ox} enriched in ^{54}Fe was converted to H_{red} with sodium dithionite in the presence of protein B.[7-11] Sample concentrations ranged from 165 μM in H and 330 μM in protein B for stopped-flow spectrophotometry to 600 μM in H and 1.2 mM in protein B for resonance Raman studies. The protein solution was mixed rapidly at 4 °C with buffer solutions saturated with $^{16}O_2$ or $^{18}O_2$ (Cambridge Isotope Labs, 97% enriched) or with $^{16}O-^{18}O$ (94 mol %).[12] These solutions were ≈1 mM in O_2 and 25 mM in MOPS, pH 7.0. Optical data were collected with a HiTech stopped-flow apparatus outfitted with a photomultiplier tube and fiber optics for monochromatic detection of absorption spectral changes at fixed wavelengths. For resonance Raman samples, the protein was mixed with dioxygen for a fixed time before being sprayed into an isopentane bath at −140 °C. The resulting snow was packed into a quartz tube in an apparatus described elsewhere.[13] The quartz tubes were transferred cold to a specially designed liquid nitrogen Raman dewar.[14] Raman spectra were obtained with excitation at 647 nm by using a Kr^+ ion laser and detected with an intensified photodiode array attached to a triple monochromator. Shifts were calibrated with CCl_4 and DMF standards. A laser power of 60 mW was employed and did not produce any photoreactions.

Stopped-flow optical spectrophotometric traces at individual wavelengths revealed a broad visible absorption for the first intermediate with $\lambda \approx 600-650$ nm ($\epsilon_{625} \approx 1500\ M^{-1}\ cm^{-1}$ per Fe_2 site).[15] These absorbance maximum and extinction coefficient values are within the range of values reported for peroxo-to-iron charge-transfer bands in several diiron(III) peroxo model complexes ($\lambda_{max} = 588-682$ nm, $\epsilon = 1300-3540\ M^{-1}\ cm^{-1}$).[16-23] A typical kinetic trace for the buildup of the intermediate, monitored at 625 nm, is given in Figure 1. Fitting these data to a first-order exponential growth curve yields a rate constant of $\approx 20\ s^{-1}$. This value is in good agreement with a kinetic analysis of the rapid freeze-quench Mössbauer data, from which a rate constant for both the growth of the intermediate and the decay of H_{red} was determined to be ≈25 s^{-1}.[4]

Rapid freeze-quench samples frozen 155 ms after mixing contained >95% of the first observed intermediate as judged by kinetic Mössbauer analysis.[15] The resonance Raman spectrum of the first intermediate excited at 647 nm (Figure 2) exhibits an isotope-sensitive feature at 905 cm^{-1} that was absent

[†] Massachusetts Institute of Technology.
[‡] Princeton University.
[§] Emory University.
[⊥] Argonne National Laboratory.

(1) Colby, J.; Dalton, H.; Whittenbury, R. *Annu. Rev. Microbiol.* **1979**, *33*, 481−517.
(2) Fox, B. G.; Froland, W. A.; Dege, J. E.; Lipscomb, J. D. *J. Biol. Chem.* **1989**, *264*, 10023−10033.
(3) Liu, K. E.; Valentine, A. M.; Wang, D.; Huynh, B. H.; Edmondson, D. E.; Salifoglou, A.; Lippard, S. J., to be submitted for publication.
(4) Liu, K. E.; Wang, D.; Huynh, B. H.; Edmondson, D. E.; Salifoglou, A.; Lippard, S. J. *J. Am. Chem. Soc.* **1994**, *116*, 7465−7466.
(5) Lee, S.-K.; Fox, B. G.; Froland, W. A.; Lipscomb, J. D.; Münck, E. *J. Am. Chem. Soc.* **1993**, *115*, 6450−6451.
(6) Lee, S.-K.; Nesheim, J. C.; Lipscomb, J. D. *J. Biol. Chem.* **1993**, *268*, 21569−21577.
(7) Proteins were purified and assayed as reported elsewhere,[8-10] with specific activities of 250−350 and 8000−8500 munit/mg for the hydroxylase and coupling protein B, respectively. The hydroxylase contained between 2.5 and 3.0 iron atoms per mole of enzyme. ^{54}Fe-enriched protein was obtained as described elsewhere.[3]
(8) Liu, K. E.; Johnson, C. C.; Newcomb, M.; Lippard, S. J. *J. Am. Chem. Soc.* **1993**, *115*, 939−947.
(9) Pilkington, S. J.; Dalton, H. *Methods In Enzymology*; Academic Press: New York, 1990; Vol. 188, pp 181−190.
(10) DeWitt, J. G.; Bentsen, J. G.; Rosenzweig, A. C.; Hedman, B.; Green, J.; Pilkington, S.; Papaefthymiou, G. C.; Dalton, H.; Hodgson, K. O.; Lippard, S. J. *J. Am. Chem. Soc.* **1991**, *113*, 9219−9235.
(11) H_{ox} was reduced in the presence of protein B, an equimolar amount of methyl viologen, and a 3-fold excess of sodium dithionite. The solution was incubated for 45 min, and the excess sodium dithionite and methyl viologen were removed during a 2-h anaerobic dialysis.
(12) Varotsis, C.; Zhang, Y.; Appelman, E. H.; Babcock, G. T. *Proc. Natl. Acad. Sci., U.S.A.* **1993**, *90*, 237−241.
(13) Ravi, N.; Bollinger, J. M., Jr.; Huynh, B. H.; Edmondson, D.; Stubbe, J. *J. Am. Chem. Soc.* **1994**, *116*, 8007−8014.
(14) Qiu, D.; Kumar, M.; Ragsdale, S. W.; Spiro, T. G. *J. Am. Chem. Soc.* **1995**, *117*, 2653−2654.
(15) This value takes into account heterogeneity in the diiron centers of MMOH from *M. capsulatus* (Bath) revealed in freeze-quench Mössbauer experiments described in detail elsewhere.[3] Briefly, our enzymatic preparations contain two types of reduced diiron clusters, $H_{red}(1)$ and $H_{red}(2)$, present in a ratio of ~1:2. Kinetic data show that $H_{red}(1)$ reacts quickly to form the intermediates, whereas $H_{red}(2)$ converts directly to H_{ox} on a time scale too slow to account for methane hydroxylation.
(16) Kitajima, N.; Tamura, N.; Amagai, H.; Fukui, H.; Moro-oka, Y.; Mizutani, Y.; Kitagawa, T.; Mathur, R.; Heerwegh, K.; Reed, C. A.; Randall, C. R.; Que, L., Jr.; Tatsumi, K. *J. Am. Chem. Soc.* **1994**, *116*, 9071−9085.
(17) Dong, Y.; Ménage, S.; Brennan, B. A.; Elgren, T. E.; Jang, H. G.; Pearce, L. L.; Que, L., Jr. *J. Am. Chem. Soc.* **1993**, *115*, 1851−1859.
(18) Hayashi, Y.; Suzuki, M.; Uehara, A.; Mizutani, Y.; Kitagawa, T. *Chem. Lett.* **1992**, 91−94.
(19) Brennan, B. A.; Chen, Q.; Juarez-Garcia, C.; True, A. E.; O'Connor, C. J.; Que, L., Jr. *Inorg. Chem.* **1991**, *30*, 1937−1943.
(20) Ménage, S.; Brennan, B. A.; Juarez-Garcia, C.; Münck, E.; Que, L., Jr. *J. Am. Chem. Soc.* **1990**, *112*, 6423−6425.
(21) Nishida, Y.; Takeuchi, M.; Shimo, H.; Kida, S. *Inorg. Chim. Acta* **1984**, *96*, 115−119.
(22) Sawyer, D. T.; McDowell, M. S.; Spencer, L.; Tsang, P. K. S. *Inorg. Chem.* **1989**, *28*, 1166−1170.
(23) Feig, A. L.; Lippard, S. J. *Chem. Rev.* **1994**, *94*, 759−805.

0002-7863/95/1517-4997$09.00/0

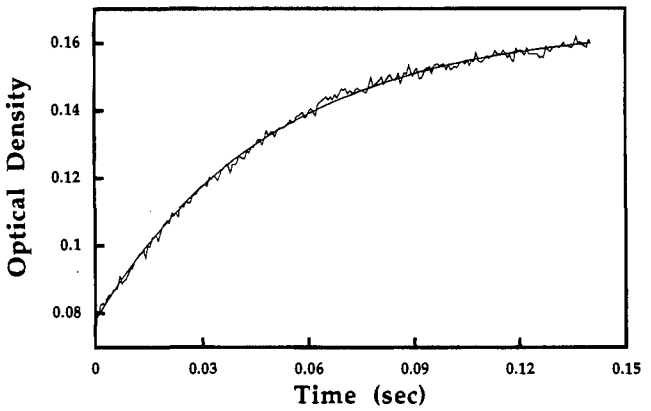

Figure 1. Time dependence of the appearance of the peroxo intermediate measured at 625 nm under pseudo-first-order conditions in dioxygen at 4 °C. A fit of the data to a first-order growth curve is superimposed, which yielded a rate constant of $k = 20\ s^{-1}$.

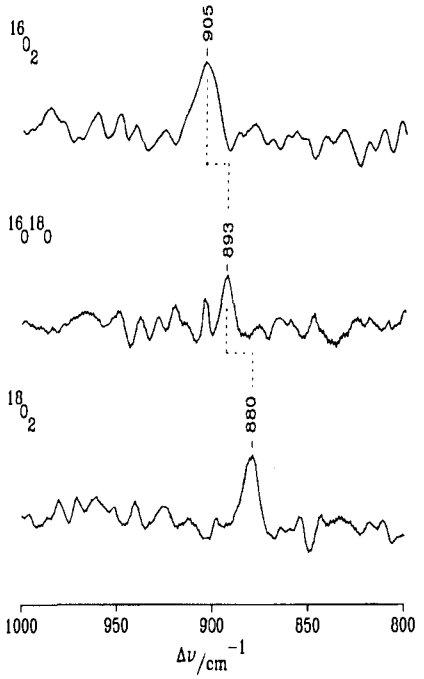

Figure 2. Rapid freeze-quench Raman spectra (647-nm excitation) of the peroxo intermediate in samples frozen 155 ms after mixing H_{red} with dioxygen ($^{16}O_2$, $^{18}O_2$, or $^{16}O-^{18}O$). The spectrum of isopentane, present in all samples prepared by the freeze-quench method, has been subtracted digitally.

in the spectra of H_{red} and H_{ox} (not shown). This value falls within the O−O stretching frequency range reported for several metal peroxo model complexes (ν(O−O) = 815−918 cm^{-1})[16-20,22-26] and is accordingly assigned as ν(O−O) of the diiron(III) peroxo unit. Excitation at 413 nm caused no enhancement of this feature, supporting the peroxo-to-Fe(III) charge-transfer assignment for the 625-nm absorption in the optical spectrum. No sensitivity to iron isotopic substitution was observed in this band. The spectrum of the sample prepared with $^{18}O_2$ indicates that ν(O−O) shifts by 25 cm^{-1} to 880 cm^{-1} upon $^{18}O_2$ substitution. Moreover, the spectrum arising from reaction with $^{16}O-^{18}O$ displays a single band at 893 cm^{-1}, halfway between the $^{16}O_2$ and $^{18}O_2$ peaks. The theoretical $^{18}O_2$ shift assuming a diatomic harmonic oscillator is −52 cm^{-1}. The reason for the smaller than expected shift is unclear but could reflect coupling of the O−O vibration to other modes in the diiron center. Vibrational coupling was recently invoked to explain a $\Delta\nu \approx 18\ cm^{-1}$ shift which occurred upon $^{18}O_2$ substitution in a PFe/Cu peroxo model complex for the dioxygen binding site in cytochrome *c* oxidase.[27] Similarly, the O−O vibration in matrix-isolated FeO_2 shifts by substantially less than the value calculated for a pure stretching mode, from 946 cm^{-1} for the $^{16}O_2$ adduct to 911 cm^{-1} for the $^{18}O_2$ derivative.[28] The fact that the present $^{16}O-^{18}O$ sample gives rise to a single Raman band indicates that the peroxo intermediate is a symmetrically bound species in which the O−O bond is still intact. The possibility remains, however, that the 893-cm^{-1} peak is an unresolved doublet, with a difference of $\leq 5\ cm^{-1}$, which could arise from an asymmetrically bound peroxide.

An oxygen-sensitive vibration between 400 and 600 cm^{-1} characteristic of ν(Fe−O_2) was not detected in the Raman spectrum. The intensity of this stretch depends on the degree to which the metal peroxo polarizability changes in the excited state. This band was not observed in several metal peroxo complexes, including oxyhemocyanin, all of which exhibit detectable ν(O−O) stretches.[29] In oxyhemocyanin, a peroxo-dicopper(II) vibration is seen at 542 cm^{-1}, in resonance with the higher energy transfer transition in the UV but not with the lower energy visible transitions.[30] Additional bands around 550 cm^{-1} do appear in the spectra of H_{ox} and H_{red} as well as that of the first intermediate (data not shown). These signals shift up in the ^{54}Fe-enriched protein and fall within the reported range for iron−oxygen stretching frequencies.[31] We tentatively attribute these Fe−O stretching modes to the coordinated glutamates.

Additional evidence for the symmetrical binding of the peroxo ligand to the diiron center is given by the narrow quadrupolar doublet lines in the Mössbauer spectrum of this intermediate.[4] This assignment suggests that the peroxo ligand coordinates in the μ-η^1:η^1 or the planar or nonplanar μ-η^2:η^2 binding mode. The *planar* μ-η^2:η^2 binding mode displayed in oxyhemocyanin and a crystallographically characterized dicopper(II) peroxo model complex has a much lower ν(O−O) stretch, $\approx$750 cm^{-1}, than observed here, however.[29,30]

In conclusion, time-resolved optical and freeze-quench resonance Raman spectroscopic experiments strongly support assignment of the first intermediate, variously designated P[6] or L,[4,32] in the MMO hydroxylase reaction cycle as a symmetrical diiron(III) peroxo species. Additional experiments are in progress to address both the coordination mode and the reactivity of the peroxo unit.

Acknowledgment. This work was supported by grants from the National Institute of General Medical Science (GM 32134 to S.J.L., GM 29433 to D.E.E., and GM 13498 to T.G.S.) and Shell (S.J.L.). Preparation of $^{16}O-^{18}O$ was carried out at Argonne National Laboratory under the auspices of the Office of Basic Energy Sciences, Division of Chemical Sciences, U.S. Department of Energy. We thank Drs. B. H. Huynh, A. Masschelein, A. Salifoglou, and Y. Wang for advice and experimental assistance, Drs. A. W. Jache and B. S. Jaynes for assistance with the preparation of the $^{16}O-^{18}O$ samples, and the referees for helpful comments.

JA943788S

(24) Murch, B. P.; Bradley, F. C.; Que, L., Jr. *J. Am. Chem. Soc.* **1986**, *108*, 5027−5028.
(25) Kitajima, N.; Fukui, H.; Moro-oka, Y. *J. Am. Chem. Soc.* **1990**, *112*, 6402−6403.
(26) Ahmad, S.; McCallum, J. D.; Shiemke, A. K.; Appelman, E. H.; Loehr, T. M.; Sanders-Loehr, J. *Inorg. Chem.* **1988**, *27*, 2230−2233.
(27) Collman, J. P.; Herrmann, P. C.; Boitrel, B.; Zhang, X.; Eberspacher, T. A.; Fu, L. *J. Am. Chem. Soc.* **1994**, *116*, 9783−9784.
(28) Abramowitz, S.; Acquista, N.; Levin, I. W. *Chem. Phys. Lett.* **1977**, *50*, 423−426.
(29) Kitajima, N.; Fujisawa, K.; Fujimoto, C.; Moro-oka, Y.; Hashimoto, S.; Kitagawa, T.; Toriumi, K.; Tatsumi, K.; Nakamura, A. *J. Am. Chem. Soc.* **1992**, *114*, 1277−1291.
(30) Ling, J.; Nestor, L. P.; Czernuszewicz, R. S.; Spiro, T. G.; Fraczkiewicz, R.; Sharma, K. D.; Loehr, T. M.; Sanders-Loehr, J. *J. Am. Chem. Soc.* **1994**, *116*, 7682−7691.
(31) Fujita, J.; Martell, A. E.; Nakamoto, K. *J. Chem. Phys.* **1962**, *36*, 324−331.
(32) We shall hereafter refer to this species as the "peroxo intermediate" rather than L.